Hydrophobic Hydration and Hydrophobic Interaction of Carboxylic Acids in Aqueous Solution: Mass Spectrometric Analysis of Liquid Fragments Isolated as Clusters

Kazunori Yamamoto and Nobuyuki Nishi*

Contribution from the Institute for Molecular Science, Myodaiji, Okazaki 444, Japan.
Received October 31, 1988

Abstract: Molecular association in aqueous solutions of some carboxylic acids was studied with mass spectrometrical analysis of cluster beams generated through adiabatic expansion of liquid jets in vacuum. This method is essentially a molecular composition analysis of frozen "fragments of liquid". The spectral pattern of the "clusters" changed depending on liquid temperatures. The change of the molecular composition was attributed to the shift of the cluster formation-dissociation equilibria in the droplets. Stability constants of κ_1 for solute monomer hydrates against pure water clusters were derived from the population ratio of the clusters. Van't Hoff plots of the stability constants provided the enthalpy changes and the entropy changes for the solute hydration process: $(H_2O)_n + RCOOH \rightleftharpoons RCOOH(H_2O)_{n-1} + H_2O$. Among six carboxylic acids investigated, the order of the stability constants κ_1 is formic < acetic < propionic < *n*-butyric < *n*-valeric < *n*-caproic acid, and the order of the enthalpies and the entropies of "hydration" is formic > acetic > propionic > *n*-butyric > *n*-valeric > *n*-caproic acid. In the formic acid system, the positive values of the enthalpy and the entropy of "hydration" are attributed to the "hydrophilic hydration" of the carboxylic groups. On the contrary, the negative enthalpies and entropies of "hydration" in the alkyl carboxylic acid systems are attributed to the "hydrophobic hydration" of the alkyl groups. The acid hydrate dimerization constant κ_D, the enthalpy of dimerization $\Delta\bar{H}_D$, and the entropy of dimerization $\Delta\bar{S}_D$ are defined for a dimerization process of acid monomer hydrates in liquid droplets: $RCOOH(H_2O)_n + RCOOH(H_2O)_{n'-1} \rightleftarrows (RCOOH)_2(H_2O)_{n-1} + (H_2O)_{n'}$. The order of the dimerization constants as well as the order of the enthalpy and the entropy of dimerization is formic < acetic < propionic < *n*-butyric < *n*-valeric < *n*-caproic acid. The chain-length dependence of the dimerization constants is thus attributed to the hydrophobic interaction between the alkyl groups. The obtained dimerization energies $\Delta\bar{H}_D$ for formic acid (0.0 kcal/mol) and acetic acid (0.0 kcal/mol) gave good agreement with the dimerization energies obtained by potentiometric titration for bulk solution of formic acid (0 ± 1 kcal/mol, ref 3) and enthalpy titration for acetic acid (0.425 ± 0.047 kcal/mol, ref 38). It was concluded that the dimerization of alkyl carboxylic acids in the aqueous systems is mainly due to entropic effect.

I. Introduction

It is well-known that carboxylic acids tend to form dimers in solutions. In nonpolar liquids such as CCl_4[1] and C_6H_6,[2] dimerization constants of the alkyl carboxylic acids are almost independent of the chain length of the alkyl residue. The results have been interpreted in terms of a cyclic dimer; i.e., the main "driving force" in the dimerization process is the formation of the two hydrogen bonds between the two solutes as shown in Figure 1a,[1-4] where nonpolar groups hardly "see" each other.

On the other hand, the dimerization in aqueous solution seems markedly different from those in the nonaqueous solvents. It was found that the dimerization constants for a homologous series of carboxylic acids in water[3,5-8] are much smaller than the corresponding values in nonpolar solvents.[1] Furthermore, it has been shown by several groups[5,7,8] that the dimerization constant in water increases with the chain length of the hydrocarbon residue. Schrier et al.[3] proposed that the dimers in water involve only one hydrogen bond (Figure 1b), and the total "driving force" for the dimerization consists of two parts: hydrogen-bond formation and hydrophobic interaction[9,10] between the alkyl groups. The latter interaction was thought to be responsible for the chain-length dependence of the dimerization constants of carboxylic acids. Unfortunately, the data available at that time were not enough to give a quantitative explanation at a molecular level. Direct conversion of liquid solution to cluster beams was developed by applying the adiabatic expansion of liquid droplets in vacuum.[11,12] This method is essentially the composition analysis of the liquid fragments and provides information on the compositional distribution of associated or clustered species in solution. Although the experimental details of the direct conversion of liquid to cluster beams was described precisely in the earlier report,[12] in order to make the understanding of the methodology more clear, the conception and the practice of the method are briefly described here.

II. Outline of the Method

How To Isolate Strongly Bound Clusters from Solution. Liquid jets emerging from a small nozzle are known to break up into many fine liquid streams, which show necking and breakup into an array of tiny droplets.[13] Introduction of these droplets into high vacuum causes immediate fragmentation to clusters and free molecules by adiabatic expansion due to the pressure change. This explosive expansion of a "superheated" liquid droplet dissociates molecules which are nonbonded or weakly bound to hydrogen-bonded clusters. This process leaves the clusters around the flight axis of the parent droplet because of their large masses relative to small masses of evaporating free molecules. The expansion process is inevitably accompanied with the evaporation of unstable surface molecules that causes substantial cooling or freezing of the fragment clusters.[14] Thus the fragments lose still more weakly bound molecules from the parent clusters. However this cooling or freezing effect also makes the intermolecular bonds of the molecules more tight so that one can know the molecular com-

(1) Wenograd, J.; Spurr, R. A. *J. Am. Chem. Soc.* **1957**, *79*, 5844.
(2) Goodmann, D. S. *J. Am. Chem. Soc.* **1958**, *80*, 3887.
(3) Schrier, E. E.; Pottle, M.; Scheraga, H. A. *J. Am. Chem. Soc.* **1964**, *86*, 3444.
(4) Murty, T. S. S. R. *J. Phys. Chem.* **1971**, *75*, 1330.
(5) Katchalsky, A.; Eisenberg, H.; Lifson, S. *J. Am. Chem. Soc.* **1951**, *73*, 5889.
(6) Cartwright, D. R.; Monk, C. B. *J. Chem. Soc.* **1955**, 2500.
(7) Carson, J. D. E.; Rossotti, F. J. C. In *Advances in the Chemistry of the Coordination Compounds*, The Macmillan Co.: New York, 1961; p 180.
(8) Mukerjee, P. *J. Phys. Chem.* **1965**, *69*, 2821.
(9) Ben-Naim, A. *Hydrophobic Interaction*; Plenum: New York, 1980.
(10) Franks, F., In *Water: A Comprehensive Treatise*: Franks, F., Ed.; Plenum: New York, 1975; Vol. 4, p 1.
(11) Nishi, N.; Yamamoto, K.; Shinohara, H.; Nagashima, U.; Okuyama, T. *Chem. Phys. Lett.* **1985**, *122*, 599.
(12) Nishi, N.; Yamamoto, K. *J. Am. Chem. Soc.* **1987**, *109*, 7353.
(13) Adamson, A. W. *Physical Chemistry of Surfaces*, 4th ed.; John Wiley & Sons: New York, 1982; pp 4-48.
(14) Klots, C. E. *J. Chem. Phys.* **1985**, *83*, 5854.

0002-7863/90/1512-549$02.50/0

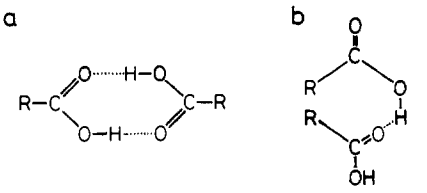

Figure 1. Two possible forms of carboxylic acid dimers from ref 9: (a) cyclic dimer and (b) open chain dimer.

position of the "surviving clusters" by mass analysis. Direct introduction of liquid to a vacuum chamber was also used by some interfaces for liquid chromatograph and mass spectrometers. One is the electrospray interface developed by Fenn and co-workers,[15] and the other is the "thermospray" interface developed by Vestal and co-workers.[16,17] Both methods share a common mechanism of "field ion desorption from liquids (FIDL)". Electrospray ionization produces atomization by charging, whereas thermospray produces charging by atomization.[15] The present neutral beam method disperses liquid into droplets by hydrodynamic forces. At a vacuum of the order of 10^{-3} Torr, these droplets situated in "superheated" states immediately cause explosive fragmentation. The fragments are quickly introduced into a high vacuum region at 10^{-7} Torr generating a cluster beam with a density on the order of $10^{-4} \sim 10^{-5}$ Torr at the electron impact ionizer.[18] When the electron beam of the mass analyzer was switched off, no ion signal was detected for distilled water and all the solutions studied so far at the maximum sensitivity of our detection system. No charging phenomenon is responsible for the beam generation. At this point, the present method is substantially different from the above two interfaces. It is interesting that the aqueous solution containing electrolyte solute showed intensity weakening of the hydrate cluster signals depending on the concentration of ionic species.[19]

From the various experimental facts reported mainly in ref 12 as well as an example shown in the Appendix, it is clear that the apparatus is looking for molecular composition of the fragments of the injected solution at the *final liquid state* before the instantaneous freezing of the binding networks of the fragments. The final liquid temperature that determines the molecular composition of the clusters was calibrated by observing the lower and the upper critical solution temperatures (LCST and UCST, respectively) of an aqueous solution of 2-butoxyethanol that shows phase separation in the range between the two critical temperatures.[12] Collisional effects around the nozzle were also examined. Increase of the pressure in the first and the second chambers not only decreased the cluster signal intensities but also made the cluster size smaller. Gas-phase collision is just destroying the clusters isolated from the liquid droplets. Fractionation of component species was not observed. For example ethyl alcohol (C_2H_5OH), which has a boiling temperature (78.3 °C at 1 atm) lower than water, and propionic acid (C_2H_5COOH), that has a boiling temperature (140.8 °C at 1 atm) higher than that of water, showed the same trend for the hydrate formation in the mass spectra indicating that gasification of a solute species with a low boiling temperature is not occurring in the course of the beam generation. The observed tendency for the hydration of the two compounds was attributed to "hydrophobic hydration" of the solute species in the aqueous systems as found by many authors in the solution systems.[20-24]

Fragmentation of Clusters on Electron-Impact Ionization. Electron impact ionization usually carries excess energy for the ionization of clusters. In the case of water clusters, it is well-known that the intensity anomalies at $H^+(H_2O)_{21}$ and $H^+(H_2O)_{28}$ evolve by metastable decay of some larger clusters after a long time delay. Echt et al. showed that these anomalies grow via evaporation of monomers mostly from 22-mer and 29-mer in the time window $4 < t < 40$ μs after ionization by electron impact.[25] The number of evaporated molecules is dependent on the intermolecular binding energies and the amount of excess energies as clearly shown by Lineburger and co-workers.[26,27] The decomposition processes of the mixed ion clusters of the type $H^+(ROH)_m(H_2O)_n$ for R = CH_3 and C_2H_5 were studied by Stace and Shukla.[28] Their analysis of metastable peaks showed the mixed ion clusters with $n > m$ evaporate one water molecule. Stace and Moore investigated the decomposition of $H^+(C_3H_7OH)_n(H_2O)$ and found that a water molecule is prefentially dissociated from the clusters with $n < 9$ which is consistent with the estimation based on RRKM theory.[29] Water clusters are known to proceed with a proton transfer reaction right after the ionization except threshold excitation.[30,31] For the electron impact at 40 eV, the ionization carries excess energy in the clusters due to the energetical difference between the Franck–Condon state and the stable ion state. In the process of the proton-transfer reaction, geometrical rearrangement around the proton is expected to occur,[32] which results in energetical stabilization due to the release of the excess energy by the evaporation of water molecule(s). Thus original neutral aqueous clusters lose at least one molecule with the ionization:

$$A_m(H_2O)_n \xrightarrow{e^-} H^+A_m(H_2O)_{n-s} + OH + (s-1)H_2O \quad (1)$$

or

$$A_m(H_2O)_n \xrightarrow{e^-} H^+A_{m-t}(H_2O)_{n-s'} + OH + (s'-1)H_2O + tA \quad (2)$$

For the clusters with $n \gg m$, process 1 is predominant, while process 2 probably takes place in the clusters with a weakly bound solute species. The adiabatic expansion process as well as the ionization process dissociates weakly bound molecules until the residual particles (or clusters) become cold enough to discontinue the dissociation in the detection time scale of $10^{-6} \sim 10^{-5}$ s. As long as the ionization is done under collision-free conditions, any compositional change except the dissociation is not expected in the aqueous systems. This is mostly due to the large heat of evaporation of liquid water.

Temperature of Liquid Droplets and Temperature of Clusters. Adiabatic expansion of *superheated* liquid droplets is not an equilibrium process at all. However, before being subject to expansion, molecules in liquid droplets are moving and exhibiting association–dissociation "reaction" at a final liquid temperature T. Now let us try to follow the fate of molecules in the solution which are flowing in the syringe needle. A typical liquid pressure in the needle is 3 atm, and the needle is usually heated at a temperature in the range 80~140 °C. When the liquid flow was stopped by closing the sample-inlet line, the needle temperature showed an immediate raise higher than 30 °C depending on the

(15) Whitehouse, C. M.; Dreyer, R. N.; Yamashita, M.; Fenn, J. B. *Anal. Chem.* **1985**, *57*, 675.
(16) Blakey, C. R.; Vestal, M. L. *Anal. Chem.* **1983**, *55*, 750.
(17) Vestal, M. L. *Science* **1984**, *226*, 275.
(18) Nishi, N.; Yamamoto, K. International School of Physics "Enrico Fermi" CVII Course, 1988, Varenna.
(19) Yamamoto, K.; Nishi, N. To be published.
(20) (a) Franks, F. In *Water: A Comprehensive Treatise*; Franks, F., Ed.; Plenum: New York, 1973; Vol. 2, Chapter 1. (b) Franks, F.; Reid, D. S. In *Water: A Comprehensive Treatise*, Franks, F., Ed.; Plenum: New York, 1973; Vol. 2, Chapter 5.
(21) Frank, H. S.; Evans, M. W. *J. Chem. Phys.* **1945**, *13*, 507.
(22) Frank, H. S.; Wen, W.-Y. *Discuss. Faraday Soc.* **1957**, *24*, 133.
(23) Nemethy, G.; Scheraga, H. A. *J. Chem. Phys.* **1962**, *36*, 3382, 3401.
(24) Nishi, N.; Koga, K.; Ohshima, C.; Yamamoto, K.; Nagashima, U.; Nagami, K. *J. Am. Chem. Soc.* **1988**, *110*, 5246.
(25) Echt, O.; Kreisle, D.; Knapp, M.; Rechnagel, E. *Chem. Phys. Lett.* **1984**, *108*, 401.
(26) Alexander, M. L.; Johnson, M. A.; Lineburger, W. C. *J. Chem. Phys.* **1985**, *82*, 5288.
(27) Levinger, N. E.; Ray, D.; Alexander, M. L.; Lineburger, W. C. *J. Chem. Phys.* **1988**, *89*, 5654.
(28) Stace, A. J.; Shukla, A. K. *J. Am. Chem. Soc.* **1982**, *104*, 5314.
(29) Stace, A. J.; Moore, C. *J. Am. Chem. Soc.* **1983**, *105*, 1814.
(30) Shinohara, H.; Nishi, N.; Washida, N. *J. Chem. Phys.* **1986**, *84*, 5561.
(31) Haberland, H.; Langosch, H. *Z. Phys. D: At., Mol. Clusters*, **1986**, *2*, 243.
(32) Hiraoka, K.; Grimsrad, E. P.; Kebarle, P. *J. Am. Chem. Soc.* **1974**, *96*, 3357.

flow rate. Clearly the flowing solution carries heat from the inner wall of the needle. This warmed solution is injected to the vacuum region through a hole of typically 40 (±15) μm forming a liquid jet stream. We know that a liquid jet emerging from a small nozzle breaks up into arrays of tiny droplets due to the instability of cylindrical columns.[13] The central part of the mist flow is introduced into the second chamber with a better vacuum (5×10^{-3} Torr) through the first skimmer. The "*superheated*" liquid particles are subject to explosion in such an isolated condition. In this course, evaporation of surface molecules may lower the temperature of liquid particles. However, molecular movement in the liquid state is rapid enough to establish "quasi-equilibrium" of association–dissociation reactions of the clusters. Such an elementary process is expected to occur within 10^{-10} s. In this paper the temperature T specifies the temperature of the final *superheated* liquid state where a considerable part of the molecules has freedom of rotational and translational motions. Since the droplets may have a wide size distribution, temperature of the droplets cannot be uniquely defined. In this sense, the temperature T, that is used for thermodynamic analysis in the later sections, should be regarded just as an averaged measure of internal energies of the various droplets. If evaporation occurs so drastically that a droplet loses freedom of molecular rotation, solidification of the droplet may occur, and the droplet may hardly exhibit adiabatic expansion any more. Expansion of liquid droplets accompanies the energy conversion of rotation and intermolecular vibration into translational motion of free molecules (and clusters). This process causes cooling of clusters. Further evaporation of free molecules from clusters accelerates the cooling. Such cooling processes are not expected to change molecular composition of strongly bound molecular clusters, since these processes just freeze the molecular motion responsible for the compositional change of clusters. The final temperatures of the clusters must be fairly lower than the temperature of the final liquid state.

The present thermodynamic analysis of the mass spectral patterns on the changes of the nozzle temperature and solute concentration is based on the above-mentioned assumption that the molecular composition of the observed clusters is originated in the local "quasi-equilibrium" in the liquid droplet state at a temperature T.

Stability Constants of Hydrate Clusters. In the previous report,[12] a stability constant κ_m of hydrate clusters $A_m(H_2O)_{n-1}$ was introduced as a form defined by the equation

$$\kappa_m = m\frac{[H^+A_m(H_2O)_{n'-1}]}{[H^+A_{m-1}(H_2O)_{n'}]}\frac{1}{(n' + n_0)}\frac{x_2}{x_1} \tag{3}$$

where x_1/x_2 is the molar ratio of solute to solvent. The constant κ_m is obtained from the slope of the plots of ion population ratio $[H^+A_m(H_2O)_{n'-1}]/[H^+A_{m-1}(H_2O)_{n'}]$ against the water numbers n'. It should be noted that the "ion population ratio" is not identical with the ratio of observed ion intensities. The observed intensities must be calibrated for electron impact ionization efficiency of the respective cluster species. For the present systems with $\Delta m = 1$ and $n' \geq 10$, the population ratios are nearly equal to the observed intensity ratios. The origin of the plots of the population ratio at the n' axis (calibrated for the ionization efficiency) gives $-n_0$. n_0 means a total number of water molecules lost from the original neutral clusters on the expansion process (loss number r) and on the ionization (loss number s). Namely, $n_0 = r + s$. As far as the experimental condition is kept constant, one can use this stability constant as a measure of the strength of the hydrate clusters. This parameter can be used irrespective of the origin of observed clusters, as long as the ion population ratio is a linear function of the hydration number $n' + n_0$.

As described above, the molecular composition of the clusters isolated from liquid jets originated in the association–dissociation equilibrium in the final liquid state of the superheated droplets. For the solute-hydrate formation in the liquid, the following molecular exchange process must be considered:

$$A_{m-1}(H_2O)_n + A \rightleftarrows A_m(H_2O)_{n-1} + H_2O \tag{4}$$

This expression is essentially based on the "flickering cluster" model[22,23] of solutions.[12] The equilibrium constant for the above process is given by the following equation:

$$K_m^n = \frac{[A_m(H_2O)_{n-1}][H_2O]}{[A_{m-1}(H_2O)_n][A]} = \frac{[A_m(H_2O)_{n-1}]}{[A_{m-1}(H_2O)_n]}\frac{x_2}{x_1} \tag{5}$$

where the concentration of free solute molecules relative to that of free solvent ones is assumed to be proportional to the molar ratio of solute to solvent (x_1/x_2) in dilute systems.

For large hydrate clusters, the evaporation number of water molecule(s) in eq 1 is considered to be constant, and the plots of the ion population ratio in eq 3 show linearity against the hydration number n. In fact, the plots showed linearity for the hydration numbers larger than 5 in most cases. Then one can write the following equation for large hydrate clusters:

$$\frac{[A(H_2O)_{n-1}]}{[(H_2O)_n]} = \frac{[H^+A(H_2O)_{n-1-n_0}]}{[H^+(H_2O)_{n-n_0}]} \tag{6}$$

$$\frac{[A_2(H_2O)_{n-1}]}{[A(H_2O)_n]} = \frac{[H^+A_2(H_2O)_{n-1-n_0}]}{[H^+A(H_2O)_{n-n_0}]} \tag{7}$$

With this condition, κ_m is related to the equilibrium constant K_m^n as follows:

$$\kappa_m = (m/n)K_m^n \tag{8}$$

This relation makes the meaning of the stability constant clear. For alcohols and carboxylic acids, the association equilibrium 4 was found to be largely shifted to the right direction, corresponding to large κ_m.[12] This indicates that those solute molecules tend to form hydrated solute oligomers. In the case of ethanol, the temperature dependence of the cluster population ratios revealed that the exchange reaction 4 is an exothermic process in dilute solutions ($\Delta H_m^n = -4.5 \pm 0.9$ kcal/mol, for $1 \leq m \leq 3$).[12,24] This enthalpy change was attributed to the hydrophobic hydration to the ethyl groups of ethanol molecules in aqueous environment, and the large κ_m values in the ethanol system were thus attributed to the large exothermicity of the association equilibrium 4.

III. Experimental Section

The apparatus and the experimental condition for generating cluster beams from liquid were the same as those reported before.[12] Aqueous solutions were converted to mist particles in the expansion chamber where the vacuum was maintained below 0.3 Torr by a liquid nitrogen trap and a rotary pump (400 L/min). A flow rate of 0.09 mL/min and nozzle-skimmer distance of 2.0 mm were adopted. After passing the first skimmer the mist particles were converted to clusters where the vacuum was maintained below 0.008 Torr by an oil diffusion ejector pump (300 L/s). Because of the very short flight path in this room (~8 mm), collisional effects on the cluster distributions were minimized. The clusters were thus immediately skimmed and introduced to the detection chamber with a vacuum lower than 2×10^{-7} Torr.

The clusters were ionized by 40 eV electron impact and analyzed by a quadrupole mass spectrometer (ANELVA AGA-360). The signals were accumulated 512 times by using a Nicolet 1170 signal averager that allowed us to measure the signal intensities at a very large dynamic range. For the comparison of the cluster intensities, mass dependence of the spectrometer sensitivity was calibrated by measuring both the spectral pattern of perfluoro-*n*-hexane[12] and the distribution of water clusters generated from neat water. In a propionic acid system, the mass numbers of $H^+C_2H_5COOH(H_2O)_{n-4}$ coincide with those of $H^+(H_2O)_{n-1}(H_2{}^{18}O)$ of which abundance relative to those of $H^+(H_2O)_n$ is precisely known. This problem happens also to the dimer hydrates of formic acid and propionic acid. In these cases, the intensities of the hydrate species were derived by subtracting the contribution of the water isotope ions.

Formic acid, acetic acid, propionic acid, *n*-butyric acid, *n*-valeric acid, and *n*-caproic acid were Tokyo Kasei's guaranteed grade and high purity water from a Mili-Q Reagent-Grade Water System was used as a solvent for excluding dust. Each carboxylic acid was mixed with water in molar ratios of 1:200–1:800, that correspond to the concentrations of 0.28–0.07 mol/L. In the range of the concentration adopted here, the contribution of ionic species to the solution structure was disregarded since the ionization constant[33] indicates that only 2.5% of solute molecules are ionized

(33) Kortüm, G.; Vogel, W.; Andrussow, K. *Dissociation Constants of Organic Acids in Aqueous Solution*; Butterworths: London, 1961.

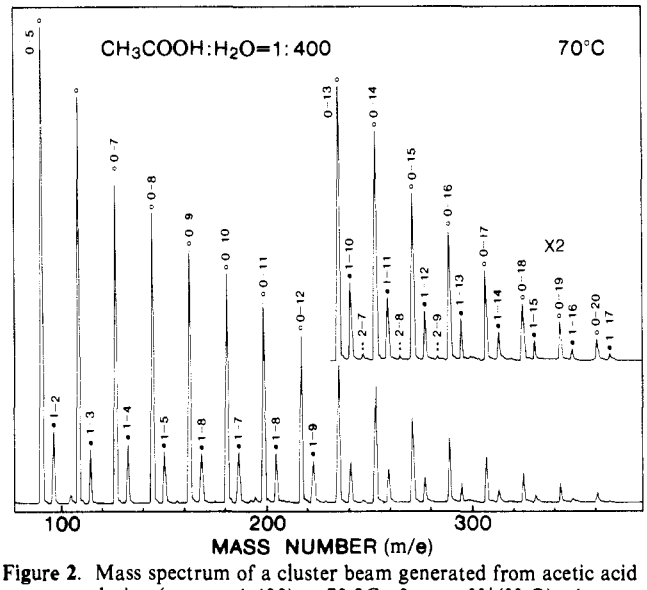

Figure 2. Mass spectrum of a cluster beam generated from acetic acid aqueous solution (x_1:x_2 = 1:400) at 70 °C. $0-n \equiv H^+(H_2O)_n$, $1-n \equiv H^+A(H_2O)_n$, and $2-n \equiv H^+A_2(H_2O)_n$. Electron impact ionization energy = 40 eV.

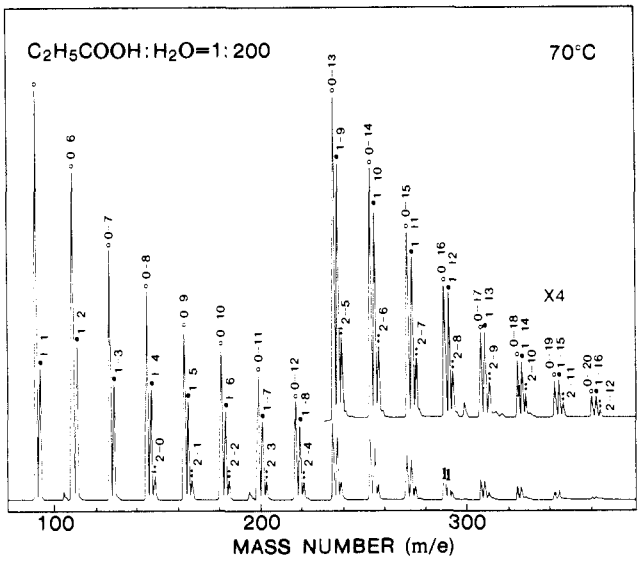

Figure 3. Mass spectrum of a cluster beam generated from propionic acid aqueous solution (x_1:x_2 = 1:200) at 70 °C. Electron impact ionization energy = 40 eV.

in an aqueous solution of formic acid (x_1 = 0.005) at 25 °C and the ion abundance for the other carboxylic acids is lower than that of the formic acid system.

Temperature dependence of the cluster distribution was measured for all the solutions. In order to know the temperature of the liquid at which the observed molecular association equilibria were maintained, we observed the two critical solution temperatures of the aqueous solution of 5% 2-butoxyethanol under the same expansion condition.[12] The temperature of the needle of the liquid nozzle was monitored at 4 mm behind the nozzle head by a thermocouple which indicated the temperatures 50–60 °C higher than those of the liquid in the range of the liquid temperatures 30–105 °C.

IV. Results

Cluster Ion Intensity Ratios and Stability of Hydrate Clusters. As reported previously,[12] the relative mass spectral intensities of formic and acetic acid monomer hydrate clusters and dimer hydrate clusters changed in direct ratio of the acid molar fraction of the binary solutions with $x_1 \leq 0.02$ at a liquid temperature of 65 °C. Figures 2–4 show the mass spectra of aqueous solutions of acetic, propionic, and *n*-valeric acids at a liquid temperature of 70 °C. Although the concentration is rather low (x_1 = 0.0025 or 0.005), one can clearly see the dimer hydrates as well as the monomer hydrates and pure water clusters. Figures 5–7 show

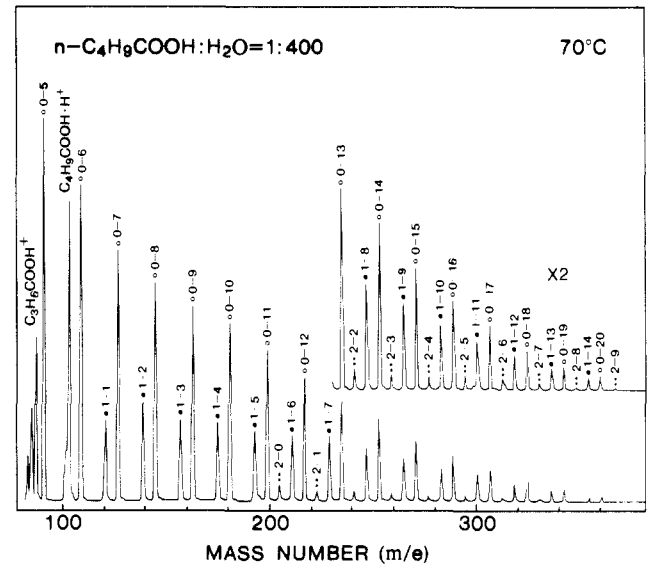

Figure 4. Mass spectrum of a cluster beam generated from *n*-valeric acid aqueous solution (x_1:x_2 = 1:400) at 70 °C. Electron impact ionization energy = 40 eV.

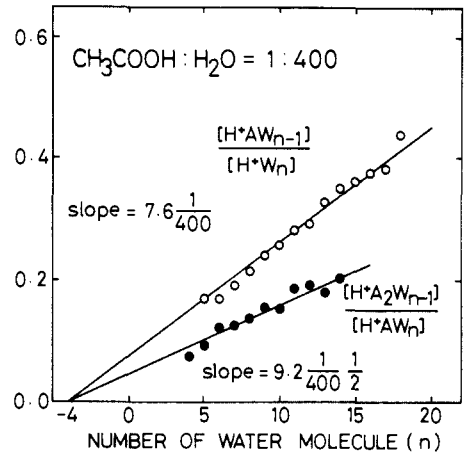

Figure 5. Plots of population ratios of acetic acid dimer hydrates to monomer hydrates ($[H^+A_2(H_2O)_{n-1}]/[H^+A(H_2O)_n]$, filled circle) and the ratio of monomer hydrates to water clusters ($[H^+A(H_2O)_{n-1}]/[H^+(H_2O)_n]$, open circle) as functions of the number of water molecules (n) observed in acetic acid aqueous solution (x_1/x_2 = 1/400). Slope values of the best fit lines are indicated.

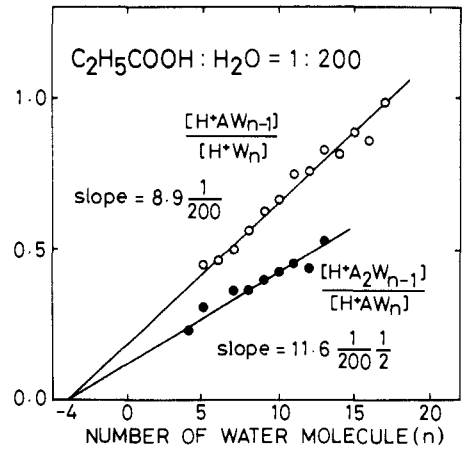

Figure 6. Plots of population ratios of propionic acid dimer hydrates to monomer hydrates (filled circle) and the ratio of monomer hydrates to water clusters (open circle) as functions of the number of water molecules (n) observed in propionic acid aqueous solution (x_1/x_2 = 1/200).

the observed population ratios of $[H^+A(H_2O)_{n-1}]/[H^+(H_2O)_n]$ and $[H^+A_2(H_2O)_{n-1}]/[H^+A(H_2O)_n]$ as functions of the number

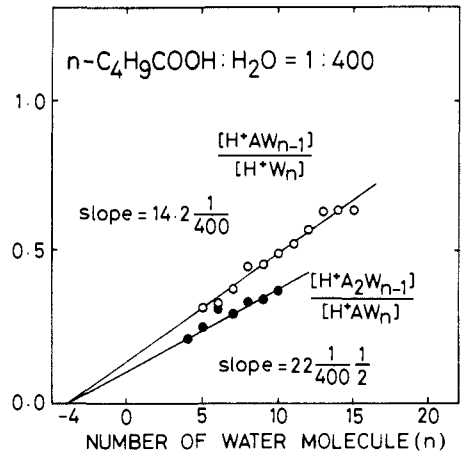

Figure 7. Plots of population ratios of *n*-valeric acid dimer hydrates to monomer hydrates (filled circle) and the ratio of monomer hydrates to water clusters (open circle) as functions of the number of water molecules (n) observed in *n*-valeric acid aqueous solution ($x_1/x_2 = 1/400$).

Table I. Stability of Monomer Hydrate Clusters (κ_1) and Dimer Hydrate Clusters (κ_2) in Aqueous Solutions Represented as Observed Abundances of the Respective Hydrate Clusters Relative to Stochstic Abundance[a]

solute species	κ_1	cluster size valid for κ_1	κ_2	cluster size valid for κ_2	κ_2/κ_1
HCOOH	6.9	$11 \le n \le 18$	6.0	$10 \le n \le 16$	0.9
CH_3COOH	7.6	$5 \le n \le 18$	9.2	$4 \le n \le 14$	1.2
C_2H_5COOH	8.9	$5 \le n \le 17$	11.6	$4 \le n \le 13$	1.3
C_3H_7COOH	12	$5 \le n \le 16$	17	$4 \le n \le 11$	1.4
C_4H_9COOH	14	$5 \le n \le 15$	22	$4 \le n \le 10$	1.5
$C_5H_{11}COOH$	17	$5 \le n \le 14$	31	$4 \le n \le 8$	1.8

[a] Temperature: 70 °C.

of water molecules n. The ratios were corrected for electron impact ionization cross section and mass dependence of the detector sensitivity. As reported before,[12] the population ratios linearly increase with increasing the water number n. The plots of $[H^+A(H_2O)_{n-1}]/[H^+(H_2O)_n]$ show a fit to a line originated at $n = -4$ in the range of $n \ge 5$ for each system as shown in Figures 5–7, which are also seen for other alkyl carboxylic acids.

The values of κ_1 and κ_2 obtained at 70 °C are listed in Table I. The stability constants of formic acid hydrates and acetic acid hydrates were redetermined. It is clearly seen that κ_1 and κ_2 depend on the chain length of alkyl group. The values of κ_1 and κ_2 clearly increase almost linearly with increasing the number of methylene groups in a molecule. The abundances of monomer hydrates for *n*-caproic acid, for example, are 17 times as strong as those expected by the stochastic distribution that assumes equivalent intermolecular interaction for all molecular pairs in the liquid. Another interesting point is that the value of κ_2/κ_1 also increases progressively with increasing chain length. For formic acid κ_2/κ_1 is 0.9, while this value is more than one for all alkyl carboxylic acids. The meaning of κ_2/κ_1 will be elucidated in a later section.

Temperature Dependence of Association Equilibria. The spectral pattern changed sensitively with increasing temperature of the liquid.[12] Figures 8–10 display the temperature dependence of the spectral patterns of the formic acid, *n*-butyric acid, and *n*-caproic acid systems. *n*-Butyric acid and *n*-caproic acid as well as other alkyl carboxylic acids showed clear temperature changes as shown in Figures 9 and 10. The pure water cluster signals were predominant at higher temperatures. At lower temperatures the cluster spectrum became more complicated, and the monomer hydrate signals were particularly prominent. This trend of the spectral change on temperature increase or decrease was similar to that observed for ethanol solutions with solute molar fractions of less than 0.12.[12,24]

As seen in Figure 8, formic acid shows temperature dependence different from alkyl carboxylic acids. Pure water clusters are more dominant at lower temperatures in contrast to the change in

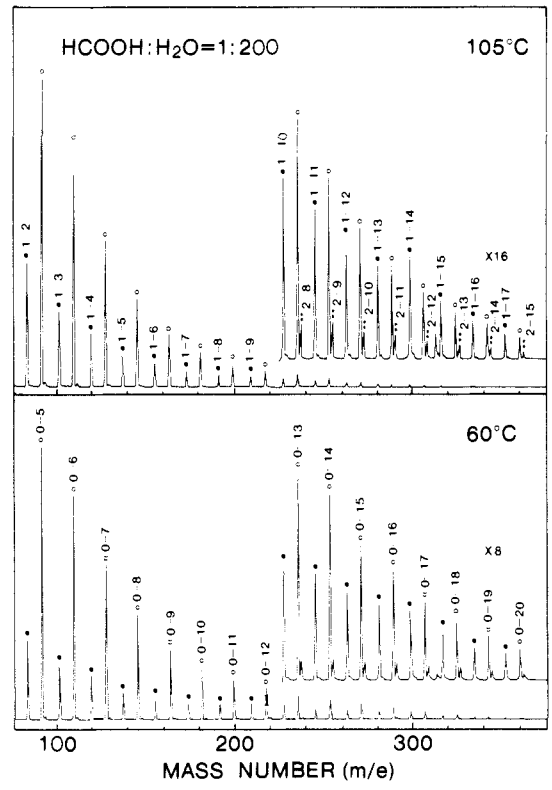

Figure 8. Temperature change of mass spectral pattern of formic acid aqueous solution ($x_1:x_2 = 1:200$) at 105 °C (top) and 60 °C (bottom). $0 - n \equiv H^+(H_2O)_n$, $1 - n \equiv H^+A(H_2O)_n$, and $2 - n \equiv H^+A_2(H_2O)_n$. Electron energy = 40 eV.

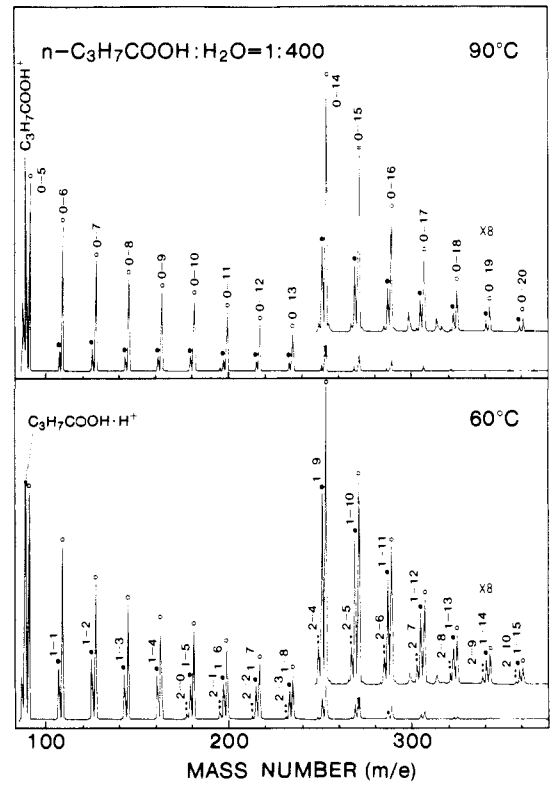

Figure 9. Temperature change of mass spectral pattern of *n*-butyric acid aqueous solution ($x_1:x_2 = 1:400$) at 90 °C (top) and 60 °C (bottom). Electron energy = 40 eV.

Figures 9 and 10, although the temperature dependence was rather small. Similar temperature changes were observed for formaldehyde[18] and formamide.

In the previous paper,[12] it was shown that van't Hoff plots of the population ratios, $[H^+A_m(H_2O)_{n-1}]/[H^+A_{m-1}(H_2O)_n]$, give

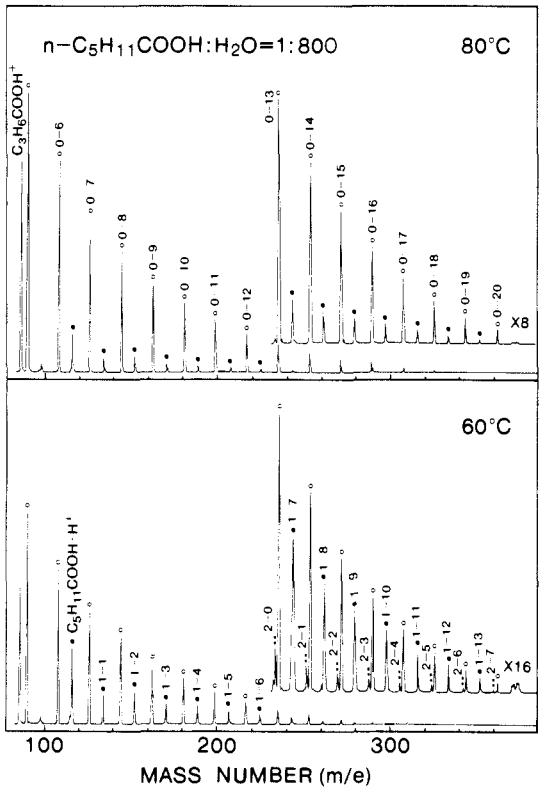

Figure 10. Temperature change of mass spectral pattern of *n*-caproic acid aqueous solution (x_1:x_2 = 1:800) at 80 °C (top) and 60 °C (bottom). Electron energy = 40 eV.

the enthalpy change of the molecular exchange process 4 based on the approximation adopted for eq 6 and 7,

$$\ln \frac{[H^+A_m(H_2O)_{n-n_0-1}]}{[H^+A_{m-1}(H_2O)_{n-n_0}]} = \ln \frac{[A_m(H_2O)_{n-1}]}{[A_{m-1}(H_2O)_n]}$$

$$= \frac{\Delta H_m^n}{R}\frac{1}{T} + \frac{\Delta S_m^n}{R} + \ln \frac{x_1}{x_2} \qquad (9)$$

where ΔH_m^n and ΔS_m^n are the enthalpy change and the entropy change of the exchange reaction 4, respectively. From eq 3 and 9, one can obtain the following relation:

$$\ln \kappa_m = -\frac{\Delta H_m^n}{R}\frac{1}{T} + \frac{1}{R}\left(\Delta S_m^n + R \ln \frac{m}{n}\right) \qquad (10)$$

Because κ_m was introduced as a parameter independent of the water number n at each temperature T, both two terms on the right hand side of eq 10 must also be independent of n. This was actually observed in the analysis with eq 9 for formic acid, acetic acid, and propionic acid. Therefore one can omit the superscript n from ΔH_m^n and express the value as $\Delta \bar{H}_m$. $R \ln (m/n)$ is a correction for the combination of solute number (m) and water number (n). Thus the entropy change $\Delta \bar{S}_m$ (independent of n) is defined as

$$\Delta \bar{S}_m = \Delta S_m^n + R \ln \frac{m}{n} \qquad (11)$$

Thus we get the following relation:

$$\ln \kappa_m = -\frac{\Delta \bar{H}_m}{R}\frac{1}{T} + \frac{\Delta \bar{S}_m}{R} \qquad (12)$$

From the temperature dependence of the stability constant κ_m, one can obtain the enthalpy change and the entropy change; $\Delta \bar{H}_m$ and $\Delta \bar{S}_m$, of the association equilibrium 4. The logarithms of the stability constants κ_1 and κ_2 are plotted against T^{-1} as shown in Figures 11 and 12. Except for formic acid, all the plots exhibit positive slopes indicating that the exchange of a water for an alkyl

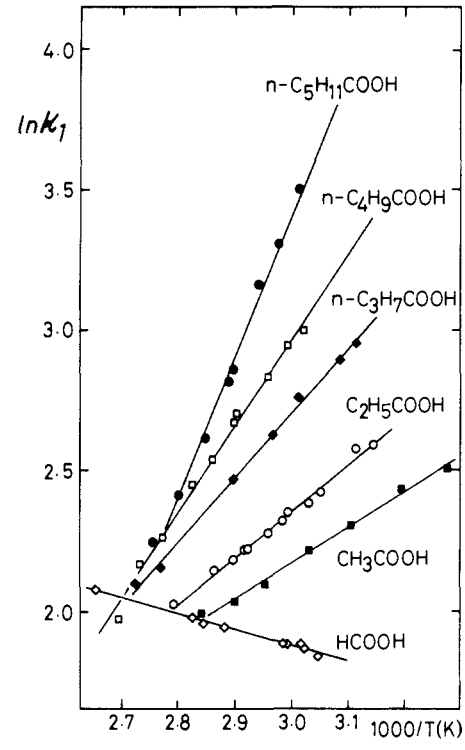

Figure 11. Logarithmic plots of κ_1 (stability constant of monomer hydrate) for six carboxylic acids as functions of T^{-1}.

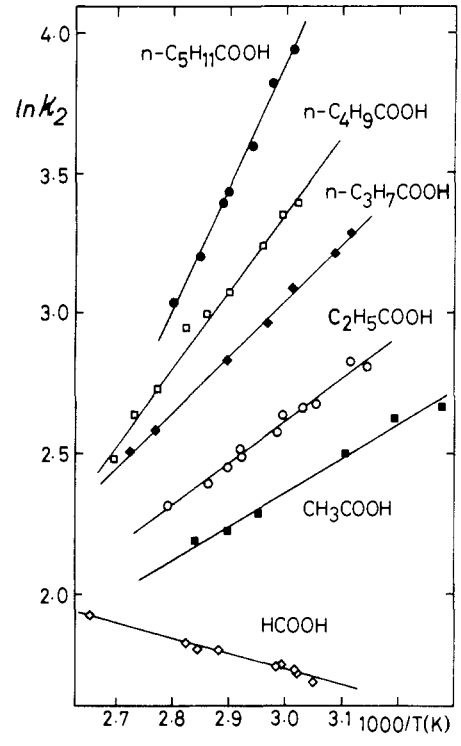

Figure 12. Logarithmic plots of κ_2 (stability constant of dimer hydrate) for six carboxylic acids as functions of T^{-1}.

carboxylic acid (expressed by eq 4) is an exothermic process in the solution. The plots for formic acid show negative slopes that mean the exchange process 4 is an endothermic reaction.

Table II displays the enthalpy changes and the entropy changes, $\Delta \bar{H}_m$ and $\Delta \bar{S}_m$ for six carboxylic acids. Formic acid shows positive values of $\Delta \bar{H}_1$ and $\Delta \bar{S}_1$, while alkyl carboxylic acids show negative values of $\Delta \bar{H}_1$ and $\Delta \bar{S}_1$. These quantities increase in absolute magnitude with an increasing number of methylene groups. Interestingly, $\Delta \bar{H}_2$ and $\Delta \bar{S}_2$ of each compound are close to the corresponding $\Delta \bar{H}_1$ and $\Delta \bar{S}_1$, respectively, but more exactly their absolute values are somewhat smaller than $\Delta \bar{H}_1$ and $\Delta \bar{S}_1$. The

Table II. Enthalpy and Entropy Changes ($\Delta\bar{H}_m$ and $\Delta\bar{S}_m$, Respectively) for the Molecular Exchange Processes: $(RCOOH)_{m-1}(H_2O)_n + RCOOH \rightleftarrows (RCOOH)_m(H_2O)_{n-1} + H_2O$ (m = 1, 2)

solute species	$\Delta\bar{H}_1$, kcal·mol^{-1}	$\Delta\bar{H}_2$, kcal·mol^{-1}	$\Delta\bar{S}_1$, cal·mol^{-1}·K^{-1}	$\Delta\bar{S}_2$, cal·mol^{-1}·K^{-1}
HCOOH	1.1	1.1	7.1	6.7
CH_3COOH	−2.3	−2.3	−2.7	−2.3
C_2H_5COOH	−3.3	−3.0	−5.1	−3.8
C_3H_7COOH	−4.5	−4.0	−8.1	−5.9
C_4H_9COOH	−6.1	−5.4	−12.3	−9.4
$C_5H_{11}COOH$	−9.7	−8.6	−22	−18

negative enthalpy change of the exchange reaction 4 was also seen in a dilute ethanol–water system (ΔH_m^n = −4.5 ± 0.9 kcal/mol).[12,24]

V. Discussion

Origin of the Stability of Carboxylic Acid Hydrates. In aqueous systems the alkyl carboxylic acids showed exothermic enthalpy changes for the processes 13 and 14, while formic acid showed endothermic changes:

$$(H_2O)_n + RCOOH \rightleftarrows RCOOH(H_2O)_{n-1} + H_2O \quad (13)$$

$$RCOOH(H_2O)_n + RCOOH \rightleftarrows (RCOOH)_2(H_2O)_{n-1} + H_2O \quad (14)$$

The enthalpy change and the entropy change, $\Delta\bar{H}_2$ and $\Delta\bar{S}_2$, for the dimer hydrate formation process 14 have the same or slightly smaller values (in absolute magnitude) as compared with $\Delta\bar{H}_1$ and $\Delta\bar{S}_1$ for the process 13 of all the carboxylic acids examined. This fact indicates that $\Delta\bar{H}_2$ and $\Delta\bar{S}_2$ mainly arise from the same factor which determines the magnitude of $\Delta\bar{H}_1$ and $\Delta\bar{S}_1$. The exothermic enthalpy changes for alkyl carboxylic acids are attributed to the formation of hydrophobic hydration regions (or shells) with orientationally ordered water molecules surrounding alkyl groups, since this ordered structure also accompanies the decreases of entropy as shown in Table II. This idea was introduced to interpret the exothermic enthalpy changes of process 4 in aqueous solutions of ethanol.[12,18,24] If the decreases of enthalpy and entropy are due to the formation of a hydrophobic hydration region, the chain length dependence of these thermodynamic properties is easily interpreted in terms of the largeness of the hydrophobic hydration region. In the exchange processes 13 and 14 the exothermic enthalpy change for alkyl carboxylic acid overcomes the loss of entropy, so that the equilibrium shifts largely to the right direction.

On the contrary, formic acid showed an endothermic enthalpy change with increasing entropy for the exchange processes 13 and 14. Similar enthalpy changes were observed for formamide and formaldehyde that have no alkyl group.[18] In formic acid the increase of entropy overcomes the endothermic enthalpy change, resulting in the shift of the equilibria 13 and 14 to the right direction. Although formic acid shows large κ_1 and κ_2 similar to those for acetic acid, the origin of the largeness is quite different from alkyl carboxylic acids. These positive enthalpy and entropy changes arise most probably from "hydrophilic hydration" composed of the hydrogen bonding between the carboxylic group and water molecules. Hydrogen bonding of pure water clusters is partially broken up by the formation of mixed clusters of the monomer hydrates in the hydration process 13. Because the molecules with the carboxylic group are essentially alien substances for water networks, they may disturb the formation of the hydrogen-bond networks of waters and, therefore, cause the total hydrogen-bond energy to decrease ($\Delta\bar{H}_1 > 0$) and the entropy to increase ($\Delta\bar{S}_1 > 0$). This disturbing effect could exist in the dimer hydrate formation process 14, but the observed changes are smaller than those of the monomer hydrate formation process 13. The perturbation of the water networks by the second solute molecule may not be as large compared with that of the first solute, judging from the $\Delta\bar{S}_2$ smaller than $\Delta\bar{S}_1$.

Table III shows the reported enthalpies of hydration of some carboxylic acids at 25 °C.[34] The initial state of the solute is gaseous in this case, while $\Delta\bar{H}_m$ or $\Delta\bar{S}_m$ in our treatment refers to the free solute molecules (with no hydrogen bond) in aqueous environment. Although the exact meaning is different, a similar trend was seen in the $\Delta\bar{H}_1$ and $\Delta\bar{H}_2$ of the present study. The enthalpy of hydration (ΔH_h^0) as well as the enthalpy change ($\Delta\bar{H}_1$ and $\Delta\bar{H}_2$) in Table II decreases as the size of the alkyl group becomes larger, although the enthalpy change $\Delta\bar{H}_1$ does not directly correspond to the enthalpy of hydration, ΔH_h^0.

Table III. Enthalpies of Hydration (ΔH_h^0) at 25 °C from Ref 34

solute species	ΔH_h^0, kcal·mol^{-1}	solute species	ΔH_h^0, kcal·mol^{-1}
HCOOH	−11.23	C_2H_5COOH	−13.50
CH_3COOH	−12.62	C_3H_7COOH	−14.22

Table IV. Enthalpy Change for the Hydrophobic Hydration to Alkyl Group[a]

side chain (R−)	$\Delta\bar{H}_1^{HH}$(R−COOH), kcal·mol^{-1}	side chain (R−)	$\Delta\bar{H}_1^{HH}$(R−COOH), kcal·mol^{-1}
CH_3−	−3.4	C_4H_9−	−7.2
C_2H_5−	−4.4	C_5H_{11}−	−11
C_3H_7−	−5.6		

[a] Temperature: 70 °C.

In order to extract information on the hydrophobic hydration, the enthalpy change for the molecular exchange process 13 is described through a simple scheme of group contributions. This method is similar to that used by Schrier[3] to extract information on the hydrophobic interaction. First it is assumed that $\Delta\bar{H}_1$ for each carboxylic acid is composed of the two contributions, one due to hydrogen-bond formation (HB) of the carboxylic group and the other one due to the hydrophobic hydration (HH) of the alkyl group:

$$\Delta\bar{H}_1(R\text{–}COOH) = \Delta\bar{H}_1^{HB}(R\text{–}COOH) + \Delta\bar{H}_1^{HH}(R\text{–}COOH) \quad (15)$$

If we assume that the hydrogen-bond formation part, $\Delta\bar{H}_1^{HB}$(R–COOH), is independent of the chain length of the alkyl group and that $\Delta\bar{H}_1$(H–COOH) has no contribution from the hydrophobic hydration, the enthalpy change for the hydrophobic hydration to an alkyl group of RCOOH, $\Delta\bar{H}_1^{HH}$(R–COOH), will be estimated as follows:

$$\Delta\bar{H}_1^{HH}(R\text{–}COOH) = \Delta\bar{H}_1(R\text{–}COOH) - \Delta\bar{H}_1(H\text{–}COOH) \quad (16)$$

A set of the enthalpies of the hydrophobic hydration for some simple alkyl groups obtained by this treatment is shown in Table IV.

The above treatment can be also applicable to the ethanol–water system studied in the previous study.[12,24] First we consider the molecular exchange process 13 for ethanol:

$$(H_2O)_n + C_2H_5OH \rightleftarrows C_2H_5OH(H_2O)_{n-1} + H_2O \quad (17)$$

The enthalpy change of process 17 is written as follows:

$$\Delta\bar{H}_1(C_2H_5\text{–}OH) = \Delta\bar{H}_1^{HB}(C_2H_5\text{–}OH) + \Delta\bar{H}_1^{HH}(C_2H_5\text{–}OH) \quad (18)$$

The major contribution to $\Delta\bar{H}_1^{HB}(C_2H_5\text{–}OH)$ is thought to be the following reactions:

$$HOH\cdots OH_2 + C_2H_5OH \rightleftarrows C_2H_5OH\cdots OH_2 + H_2O \quad (19)$$

$$HOH\cdots OH_2 + C_2H_5OH \rightleftarrows HOH\cdots OHC_2H_5 + H_2O \quad (20)$$

These processes contain the formation of some hydrogen bond and the dissociation of another set. Since the stabilization energy of the hydrogen bonds among water and ethanol are nearly the same,[24,35] the enthalpy change for eq 19 and 20, $\Delta\bar{H}_1^{HB}(C_2H_5\text{–}$

(34) Cabani, S.; Gianni, P.; Mollica, V.; Lepori, L. *J. Sol. Chem.* **1981**, *10*, 563.
(35) Curtiss, L. A.; Blander, M. *Chem. Rev.* **1988**, *88*, 827.

OH), is expected to be nearly zero. Therefore $\Delta\bar{H}_1(C_2H_5\text{–}OH)$ could be nearly equal to $\Delta\bar{H}_1^{HH}(C_2H_5\text{–}OH)$. It is reasonable that the obtained enthalpy of hydrophobic hydration increases (in absolute magnitude) with an increasing number of methylene groups in Table IV. We reported $\Delta\bar{H}_1^{HH}(C_2H_5\text{–}OH) = -4.5$ kcal/mol.[12] The present study gave $\Delta\bar{H}_1^{HH}(C_2H_5\text{–}COOH) = -4.4$ kcal/mol. We think the difference is not so great considering the experimental error of ±0.5 kcal/mol.[12] Thus, the division of the enthalpy change into the two parts in terms of eq 15 could be a reasonable approximation.

The Carboxylic Acid Dimer Formation and Hydrophobic Interaction. In this section we will discuss the dimerization of carboxylic acids in aqueous solutions, which is the core of the whole study. First we consider the dimer hydrate formation process 14. The differences in the enthalpy changes ($\Delta\bar{H}_2$ and $\Delta\bar{H}_1$) and the entropy changes ($\Delta\bar{S}_2$ and $\Delta\bar{S}_1$) are attributed to the solute–solute interaction. Following the idea given by Scheraga et al.,[36,37] we divide the enthalpy change and the entropy change in process 14 into the solute-water (S–W) and the solute–solute (S–S) parts:

$$\Delta\bar{H}_2 = \Delta\bar{H}_2^{S\text{-}W} + \Delta\bar{H}_2^{S\text{-}S} \quad (21)$$

$$\Delta\bar{S}_2 = \Delta\bar{S}_2^{S\text{-}W} + \Delta\bar{S}_2^{S\text{-}S} \quad (22)$$

Here the solute–solute interaction part contains indirect effects produced by the interaction through water molecule(s). In order to extract information on the solute–solute interaction, the solute–water interaction terms, $\Delta\bar{H}_2^{S\text{-}W}$ and $\Delta\bar{S}_2^{S\text{-}W}$, are assumed to be equivalent to the enthalpy and entropy changes of $\Delta\bar{H}_1$ and $\Delta\bar{S}_1$, respectively, for the monomer hydrate formation process 13:

$$\Delta\bar{H}_2^{S\text{-}W} = \Delta\bar{H}_1 \quad (23)$$

$$\Delta\bar{S}_2^{S\text{-}W} = \Delta\bar{S}_1 \quad (24)$$

Then we obtain

$$\Delta\bar{H}_2^{S\text{-}S} = \Delta\bar{H}_2 - \Delta\bar{H}_1 \quad (25)$$

$$\Delta\bar{S}_2^{S\text{-}S} = \Delta\bar{S}_2 - \Delta\bar{S}_1 \quad (26)$$

The above series of assumptions leads to an estimate of the contribution of the solute–solute interaction.

The introduction of the assumptions in eq 21–24 is essentially equivalent to considering the following process 27 in order to extract the pure solute–solute interaction. Although eq 27 neglects

$$RCOOH(H_2O)_n + RCOOH(H_2O)_{n'-1} \rightleftarrows (RCOOH)_2(H_2O)_{n-1} + (H_2O)_{n'} \quad (27)$$

the acid monomer and dimer species having no hydrogen bond with water, it may describe the acid dimerization process in the solution more properly. In a special case of $n' = 1$, eq 27 is equivalent to eq 14. Note that the cluster species in eq 27 are also participating in various association equilibria such as molecular exchange, dissociation, and attachment "reactions". Equation 27 is obtained by combining eq 13 and 14; therefore we define the thermodynamic properties, κ_D, $\Delta\bar{H}_D$, and $\Delta\bar{S}_D$ for process 27 which are related to those for eq 13 and 14 as follows:

$$\Delta\bar{H}_D = \Delta H_D^{n,n'} = \Delta\bar{H}_2 - \Delta\bar{H}_1 \quad (28)$$

$$\Delta\bar{S}_D = \Delta S_D^{n,n'} + R \ln \frac{2n'}{n} = \Delta\bar{S}_2 - \Delta\bar{S}_1 \quad (29)$$

$$\kappa_D = \frac{2n'}{n} K_D^{n,n'} = \frac{2n'}{n} \frac{[(RCOOH)_2(H_2O)_{n-1}][(H_2O)_{n'}]}{[RCOOH(H_2O)_n][RCOOH(H_2O)_{n'-1}]} = \frac{\kappa_2}{\kappa_1} \quad (30)$$

$$\ln \kappa_D = -\frac{\Delta\bar{H}_D}{R}\frac{1}{T} + \frac{\Delta\bar{S}_D}{R} \quad (31)$$

(36) Schneider, H.; Kresheck, G. C.; Scheraga, H. A. *J. Phys. Chem.* **1965**, *69*, 1310.
(37) Kunimitsu, D. K.; Woody, A. Y.; Stimson, E. R.; Scheraga, H. A. *J. Phys. Chem.* **1968**, *72*, 856.

Table V. Stability Constant (κ_D), Enthalpy Change ($\Delta\bar{H}_D$), and Entropy Change ($\Delta\bar{S}_D$) for the Acid Dimerization Process: $RCOOH(H_2O)_n + RCOOH(H_2O)_{n'-1} \rightleftarrows (RCOOH)_2(H_2O)_{n-1} + (H_2O)_n$

solute species	κ_D (70 °C)	$\Delta\bar{H}_D$, kcal·mol^{-1}	$\Delta\bar{S}_D$, cal·mol^{-1} K^{-1}
HCOOH	0.9	0.0	−0.4
CH_3COOH	1.2	0.0	0.4
C_2H_5COOH	1.3	0.3	1.4
C_3H_7COOH	1.4	0.5	2.2
C_4H_9COOH	1.5	0.7	2.9
$C_5H_{11}COOH$	1.8	1.1	4.2

where $K_D^{n,n'}$, $\Delta H_D^{n,n'}$, and $\Delta S_D^{n,n'}$ denote the equilibrium constant, the enthalpy change, and the entropy change for the equilibrium process 27. If the solute–solute interaction is the same as the solute–water interaction, κ_D has a value of unity. Note that κ_D, $\Delta\bar{H}_D$, and $\Delta\bar{S}_D$ are independent of the hydration numbers n and n'.

The three thermodynamic properties obtained from this treatment are given in Table V. It shows the increasing enthalpy and entropy of dimerization as the alkyl chain becomes larger. Dimerization process 27 for formic acid exhibited zero enthalpy change and negative entropy change. The enthalpy of acetic acid dimerization is also zero, while small endothermic enthalpy changes were observed for the alkyl carboxylic acids larger than acetic acid. All the alkyl carboxylic acids showed positive entropy changes of dimerization. Apparently both the enthalpy and the entropy of dimerization become larger with an increasing number of methylene groups of the alkyl residue.

Our result of $\Delta\bar{H}_D = 0.0$ kcal/mol for the dimerization of formic acid is consistent with the result of $\Delta H_D = 0 \pm 1$ kcal/mol obtained from the potentiometric titration experiments by Schrier et al.[3] For acetic acid, our value of $\Delta\bar{H}_D = 0.0$ kcal/mol is nearly equal to $\Delta H_D = 0.425 \pm 0.047$ kcal/mol obtained by Martin and Rossotti from enthalpy titration measurements.[38] The temperature dependence for the dimerization of acetic acid, propionic acid, and *N*-butyric acid obtained by Nash and Monk[39] leads to the value of $\Delta H_D = 0 \pm 1$ kcal/mol.[3] The rather small enthalpies of dimerization for carboxylic acids have been interpreted intuitively. The equilibrium 27 involves the formation of one set of hydrogen bonds with the concomitant destruction of another set[3,4]

$$R(HO)C{=}O\cdots HOH + R(O{=})C\text{—}OH\cdots OH_2 \rightleftarrows R(HO)C{=}O\cdots HO\text{—}C(=O)R + HOH\cdots OH_2 \quad (32)$$

and both sets have the total energy of hydrogen bonds with nearly the same magnitude.

The conventional dimerization constant K_D is defined for the process

$$2A \rightleftarrows A_2 \quad (33)$$

by the relation

$$K_D = C_D/C_M^2 \quad (34)$$

where C_M and C_D are the "total" concentration of the carboxylic acid monomers and dimers in solution and are expressed by the summation of related molecular species (clusters) as follows:

$$C_M = [A] + [AW] + [AW_2] + [AW_3] + \ldots \quad (35)$$

$$C_D = [A_2] + [A_2W] + [A_2W_2] + [A_2W_3] + \ldots \quad (36)$$

where $W = H_2O$. If we assume that eq 3 and 5–8 stand for all n, although this assumption is not good for $n < 5$, we obtain

$$C_M = \kappa_1 \frac{[A]}{[W]} \sum_{n=1}^{\infty} n[W_n] \quad (37)$$

$$C_D = \kappa_1\kappa_2 \frac{[A]^2}{[W]^2} \sum_{n=1}^{\infty} \frac{n(n+1)}{2}[W_n] \quad (38)$$

(38) Martin, D. L.; Rossotti, F. J. C. *Proc. Chem. Soc., London* **1961**, 73.
(39) Nash, G. R.; Monk, C. B. *J. Chem. Soc.* **1957**, 4274.

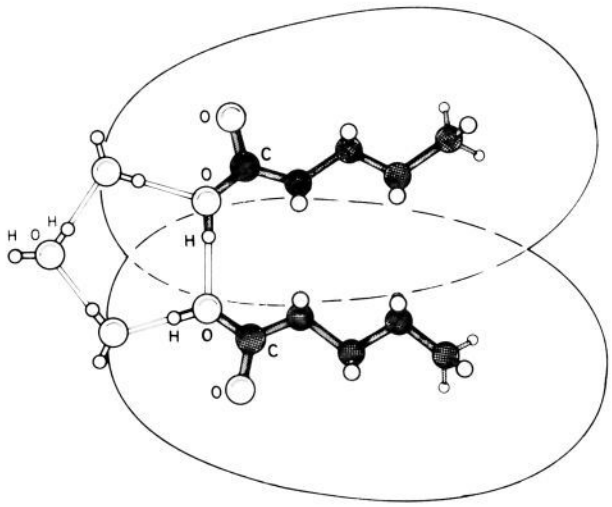

Figure 13. A model of aliphatic carboxylic acid dimer in aqueous solution. The two carboxylic groups may form a pentagonal ring with three water molecules. Hydrophobic hydration region surrounding the alkyl group is shown by ellipsoidal circles.

Table VI. Cluster Population Ratios and Stability Constant κ_1 for Solute Monomer Hydrate Against Pure Water Clusters in the Clusters from Propionic Acid Aqueous Solutions[c] at ~55 °C

x_1/x_2[a]	$([H^+C_2H_5COOH(H_2O)_{n-1}]/[H^+(H_2O)_n](n+n_0)) \times 10^3$	κ_1
0.000 67	8.6 ± 1.1[b]	12.9 ± 1.7[b]
0.001 00	12.9 ± 1.1	12.9 ± 1.1
0.001 25	16.5 ± 1.0	13.2 ± 0.8
0.002 50	30.2 ± 0.9	12.1 ± 0.4
0.005 00	55.4 ± 1.9	11.1 ± 0.4

[a] Molar ratio of solvent to solute. [b] Standard deviation. [c] Molar ratio: C_2H_5COOH/H_2O = 1/1500, 1/1000, 1/800, 1/400, and 1/200.

Therefore the conventional dimerization constant K_D is expressed by the relation

$$K_D = \kappa_D B([W_n]) \tag{39}$$

where

$$B([W_n]) = \frac{\sum_{n=1}^{\infty} \frac{n(n+1)}{2}[W_n]}{(\sum_{n=1}^{\infty} n[W_n])^2} \tag{40}$$

Relation 39 indicates that the dimerization constant K_D contains the coefficient $B([W_n])$ that is independent of the concentration of acid monomer and dimer species as a matter of form.

The increase of entropy for process 27 exceeds the contribution of the endothermic enthalpy change to the free energy (or the equilibrium constant) for propionic, *n*-butyric, *n*-valeric, and *n*-caproic acids. Therefore the equilibrium 27 shifts to the right direction for all alkyl carboxylic acids. The fact that alkyl carboxylic acids have the tendency for self-association in aqueous solution has been thought to be due to the "hydrophobic interaction" between the alkyl groups.[3,9,10] This study revealed that *the enthalpy change and the entropy change for the solute–solute interaction of alkyl carboxylic acids are positive, but those quantities for hydrophobic hydration are negative.* This trend was expected by Ben-Naim[9] from the data of Nash and Monk.[39] Therefore we conclude that the dimerization of alkyl carboxylic acids in aqueous solution is purely an "entropic effect". The chain length dependence of the entropy change (and enthalpy change) is interpreted in terms of the size of overlapping volume of the two hydrophobic hydration regions, leading to the decrease of the total volume of the two hydrophobic hydration regions. The observed trend of the dimerization of alkyl carboxylic acids is, therefore, attributed to the "hydrophobic interaction" between the alkyl groups which are surrounded by the hydrophobic hydration regions.

Table VII. Dimerization Constants of Propionic Acid Obtained in Various Investigations

	log K_D	phase	temp, °C
1[a]	−0.4[b]	water cluster	55
2	−0.50[b]	H_2O solution	25
3	−0.64[c]	H_2O solution	25
4	−1.01[c]	H_2O solution	25
4	−0.94[c]	H_2O solution	45
5	3.39[b]	CCl_4 solution	24
6	4.52[b]	gas	25
6	3.50[b]	gas	55

[a] Line head numbers refer to the works from which the data were obtained: (1) this work, (2) Carson and Rossotti,[7] (3) Katchalsky, Eisenberg, and Lifson,[5] (4) Nash and Monk,[39] (5) Wenograd and Spurr,[1] and (6) Taylor and Bruton.[40] [b] $K_D = [C((C_2H_5COOH)_2)]/[C(C_2H_5COOH)]^2$ (L/mol). [c] $^TK_D = [a((C_2H_5COOH)_2)]/[a-(C_2H_5COOH)]^2$ (L/mol).

On the basis of the present analysis, we propose a model of the dimer structure of aliphatic carboxylic acids in aqueous solution as shown in Figure 13. The two –COOH groups are probably stabilized by a pentagonal water network that will be strengthened by ionic character of the carboxylic groups. Hydrophobic hydration region is shown in the figure. Hydrogen bonding in the overlapping region could be somewhat flexible.

Appendix

Estimation of Conventional Dimerization Constants. Here the "conventional" dimerization constant (K_D) of propionic acid estimated from the cluster spectra is compared with the reported values obtained by other techniques. Cluster mass spectra of the aqueous solutions with the molar ratios of C_2H_5COOH/H_2O = 1:200, 1:400, 1:800, 1:1000, and 1:1500 at a liquid temperature of ~55 °C were measured at the same condition. Since the ratio of ionized solute molecules to neutral ones in H_2O is less than 2%, we neglected the contribution from the ionized species in the analysis. The same way as described in the paper was applied to obtain the population ratio, $[H^+C_2H_5COOH(H_2O)_{n-1}]/[H^+(H_2O)_n]$, which relates to the stability constant of monomer hydrate clusters κ_1 as follows:

$$\frac{[H^+C_2H_5COOH(H_2O)_{n-1}]}{[H^+(H_2O)_n]} = \frac{[C_2H_5COOH(H_2O)_{n-1+n_0}]}{[(H_2O)_{n+n_0}]} = \kappa_1(n+n_0)\frac{x_1}{x_2} \tag{41}$$

where x_1/x_2 is the molar ratio of solute to solvent and n_0 is the evaporation number of water molecules from parent neutral clusters. Table VI shows the observed population ratios and κ_1 at the various concentrations. The population ratio (left hand side of eq 41) was actually found to be proportional to the molar ratio x_1/x_2 only in the concentration region of $x_1/x_2 \leq 0.001\,25$. This was elucidated by regarding the solution in this dilute region as a "solute-monomer solution" where the solute polymer is negligible. In fact dimer hydrates were not seen in the mass spectra of the solutions, and κ_1 was constant and independent of x_1/x_2 in this concentration region. At higher concentrations ($x_1/x_2 \geq 0.0025$), κ_1 is a function of x_1/x_2 due to solute–solute association which leads to the decrease of monomer species in the solutions. Acid dimer hydrate and even the trimer hydrate clusters were observed at $x_1/x_2 = 0.005$. Since acid dimer hydrate clusters are the main polymer species at $x_1/x_2 = 0.0025$, the decrease in κ_1 is attributed to the formation of the dimer species only. Therefore, one can estimate the dimer fraction x_D of propionic acid at $x_1/x_2 = 0.0025$ (0.137 mol/L) as follows:

$$x_D = \frac{\kappa_1(x_1/x_2 = 0.001\,25) - \kappa_1(x_1/x_2 = 0.0025)}{\kappa_1(x_1/x_2 = 0.001\,25)} = 0.088 \pm 0.070 \tag{42}$$

The conventional dimerization constant for $2C_2H_5COOH \rightleftarrows (C_2H_5COOH)_2$ was given by

$$K_D = \frac{C_D}{(C - C_D)^2} = \frac{x_D}{2C(1 - x_D)^2} \quad (43)$$

where C is the total acid concentration, and C_D ($=x_DC/2$) is the concentration of acid dimer. Note that our discussion outlined above is also valid when we use a simple "intensity ratio" $[H^+C_2H_5COOH(H_2O)_{n-1}]/[H^+(H_2O)_n]$ instead of the population ratio (left hand side of eq 4) that was derived by calibrating electron impact ionization cross section, mass dependence of the mass spectrometer, and the cluster size distribution of the beams.

Table VII presents a compilation of the result with some dimerization constants in solutions as well as those in the gas phase. The present K_D value obtained from the cluster distribution is close to the values obtained by other measurements such as potentiometric titration of bulk aqueous solution. The small difference between our result of log $K_D = -0.4$ and the other results of log ${}^TK_D = -0.64$ to -1.01 (line numbers 3 and 4 in Table VII) may be explained mainly by the difference of the definition of the dimerization constant. ${}^TK_D$ were defined by the activities of the solutes (${}^TK_D = [a(A_2)]/[a(A)]^2$) where $a(A_2)$ and $a(A)$ are the activities of solute dimer and solute monomer, respectively. The slight difference between our result (log $K_D = -0.4$) and the value from Carson and Rossotti[7] (log $K_D = -0.50$) may be explained by the difference of the solution temperatures (55 °C and 25 °C). Temperature dependence of K_D for propionic acid is expected to be small and positive for the temperature increase because the enthalpy of dimerization (ΔH_D) in H_2O is 0.4 kcal/mol for acetic acid.[38] The dimerization constant in the gas phase[40] is more than 10^4 greater than those in aqueous solution.[7] The coincidence of dimerization constants of propionic acid both in bulk solution and in the isolated clusters confirmed that *the compositions of the clusters separated from aqueous solutions reflect the association properties in the original solutions.*

Registry No. HCOOH, 64-18-6; CH_3COOH, 64-19-7; C_2H_5COOH, 79-09-4; C_3H_7COOH, 107-92-6; C_4H_9COOH, 109-52-4; $C_5H_{11}COOH$, 142-62-1; H_2O, 7732-18-5.

(40) Taylor, M. D.; Bruton, J. *J. Am. Chem. Soc.* **1952**, *74*, 4151.

Fundamental Studies of Microscopic Wetting on Organic Surfaces. 1. Formation and Structural Characterization of a Self-Consistent Series of Polyfunctional Organic Monolayers

Ralph G. Nuzzo,*,† Lawrence H. Dubois,*,† and David L. Allara*,‡

Contribution from the AT&T Bell Laboratories, Murray Hill, New Jersey 07974, and Departments of Chemistry and Materials Science and Engineering, Pennsylvania State University, University Park, Pennsylvania 16802. *Received February 17, 1989*

Abstract: Monolayers of a series of terminally substituted alkyl thiols, $X(CH_2)_{15}SH$ (X = CH_3, CH_2OH, CO_2H, CO_2CH_3, and $CONH_2$), have been prepared by adsorption from solution onto evaporated gold substrates. The structures have been characterized by infrared (IR) spectroscopy, X-ray photoelectron spectroscopy (XPS), ellipsometry, and temperature-programmed desorption (TPD). The IR data shows the monolayer films to be densely packed, crystalline-like structures with all-trans conformation alkyl chains exhibiting average tilt angles of the chain axis in a range of 28-40° from the surface normal and an approximate 55° twist of the chain axis away from a configuration with the CCC plane perpendicular to the surface plane. TPD results set a lower limit of interaction between the CH_2 groups in the films of ~0.8 kcal/mol. We find that the terminal groups are exposed at the ambient interface, and, based on an analysis of the IR data, an assessment of the conformations and molecular environments of these groups is made. The CO_2H terminal groups appear to exist in short hydrogen-bonded (perhaps dimeric) sequences. Detailed examination of the IR data shows some unexplained abnormalities with respect to the quantitative treatment of the terminal functional group spectra. These effects can be traced to the perturbations which occur when a group is placed at an interface relative to the environment experienced in a crystalline solid. The major feature of this study is the finding that the reported series of derivatives form a structurally self-consistent set of well-defined reagent surfaces suitable for use in further studies of the surface properties of organic materials.

The chemisorption of organosulfur compounds on gold surfaces has proven to be a remarkably useful and powerful synthetic methodology for the construction of well-defined organic surfaces and interfaces.[1-9] Recent papers have established the general characteristics of the surface phases obtained with several structurally diverse adsorbate systems, in particular simple aliphatic and certain substituted disulfides,[1,3,4] the *n*-alkyl thiols,[5,10] and a broad range of symmetrical and unsymmetrical dialkylsulfides.[2] Diffraction studies have also demonstrated ordering in certain phases formed from long-chain *n*-alkyl thiols.[11] Whitesides and co-workers have detailed structural relationships in wetting behavior by using this chemisorption system.[2,5-7,9] Similar relationships were also established in UHV chemisorption studies by Dubois et al.[12] The combined weight of this reported work establishes several important general principles. First, when

Scheme I

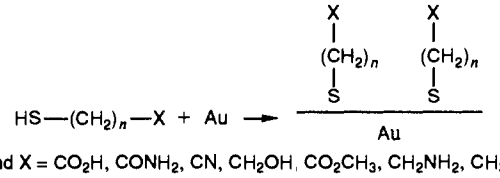

($n \geq 1$ and X = CO_2H, $CONH_2$, CN, CH_2OH, CO_2CH_3, CH_2NH_2, CH_3, $CHCH_2$, etc.)

† AT&T Bell Laboratories.
‡ Pennsylvania State University.

(1) Nuzzo, R. G.; Allara, D. L. *J. Am. Chem. Soc.* **1983**, *105*, 4481-83.
(2) Troughton, E. B.; Bain, C. D.; Whitesides, G. M.; Nuzzo, R. G.; Allara, D. L.; Porter, M. D. *Langmuir* **1988**, *4*, 365-385.

0002-7863/90/1512-558$02.50/0